Trapezoid mesa trench metal–oxide semiconductor barrier Schottky rectifier: an improved Schottky rectifier with better reverse characteristics*

Li Wei-Yi(李惟一), Ru Guo-Ping(茹国平)†, Jiang Yu-Long(蒋玉龙), and Ruan Gang(阮 刚)

State Key Laboratory of ASIC and System, Department of Microelectronics, Fudan University, Shanghai 200433, *China*

(Received 7 December 2010; revised manuscript received 28 April 2011)

An improved structure of Schottky rectifier, called a trapezoid mesa trench metal–oxide semiconductor (MOS) barrier Schottky rectifier (TM-TMBS), is proposed and studied by two-dimensional numerical simulations. Both forward and especially better reverse I–V characteristics, including lower leakage current and higher breakdown voltage, are demonstrated by comparing our proposed TM-TMBS with a regular trench MOS barrier Schottky rectifier (TMBS) as well as a conventional planar Schottky barrier diode rectifier. Optimized device parameters corresponding to the requirement for high breakdown voltage are given. With optimized parameters, TM-TMBS attains a breakdown voltage of 186 V, which is 6.3% larger than that of the optimized TMBS, and a leakage current of 4.3×10^{-6} A/cm^2, which is 26% smaller than that of the optimized TMBS. The relationship between optimized breakdown voltage and some device parameters is studied. Explanations and design rules are given according to this relationship.

Keywords: Schottky rectifier, pinch-off effect, breakdown, power device

PACS: 73.30.+y, 73.40.Ei, 73.40.Qv, 85.30.De **DOI:** 10.1088/1674-1056/20/8/087304

1. Introduction

The Schottky barrier diode (SBD) is widely used as a rectifier in industrial applications. Compared with a P–i–N rectifier, SBD has advantages mainly of low forward drop and faster reverse recovery. Basically, an SBD is expected to have low forward voltage drop and low reverse leakage current, which lead to low power dissipation. However, the tradeoff between these two factors makes it difficult to achieve these characteristics simultaneously.[1] In addition, for the application to a power device, a higher breakdown voltage is required. For a conventional planar SBD, a relatively small Schottky barrier height (SBH) and a relatively high doping concentration lead to low forward voltage drop but high reverse leakage current and low breakdown voltage, and *vice versa*.[2] To reduce the reverse leakage current as well as to raise the breakdown voltage, different structures of SBD, such as a junction-barrier-controlled Schottky rectifier,[3−6] merged P–i–N Schottky rectifier,[7,8] trench MOS barrier Schottky rectifier (TMBS),[9−16] and dual-metal-trench Schottky pinch-rectifier,[17−19] have been proposed and discussed. The TMBS was regarded as a possible candidate that meets the above requirements. Some advanced work on experiments[10−13] and simulations[14−16] has been done to improve the characteristics of the TMBS. It was mentioned that the breakdown of a TMBS occurs near the bottom of the trench.[9] However, as revealed in our previous work,[20] the field crowding near the trench corner of the TMBS causes the difficulty in achieving a more uniform electric field, thus a higher breakdown voltage. In this work, enlightened by the improved design of the UMOS power device,[21] we propose an improved TMBS structure—trapezoid mesa TMBS (TM-TMBS) to restrain the high electric field peak at the corner, thus to achieve better reverse characteristics.

2. Device structure

The structure of the TM-TMBS is schematically shown in Fig. 1(a), in which a is the mesa top width, b is the mesa bottom width, c is the N^- epi layer thickness, d is the trench depth, s is the space between two mesa tops, γ is the tilt angle of the mesa region, and t_{ox} is the oxide thickness. The anode electrode metal that fills the trench region forms a Schottky contact

*Project supported by the International Research Training Group "Materials and Concepts for Interconnects and Nanosystems".
†Corresponding author. E-mail: gpru@fudan.edu.cn
© 2011 Chinese Physical Society and IOP Publishing Ltd

with the silicon mesa. This contact can also be formed by an appropriate silicide instead of metal. The cathode contact is Ohmic. The key feature of this device is the trapezoid mesa region, which leads to tilted MOS sidewalls, compared with the rectangular mesa region of the TMBS.[9] This difference is expected to reduce the field magnitude peak values at the bottom corners of the mesa region. For comparison, the structure of the TMBS is also shown in Fig. 1(b).

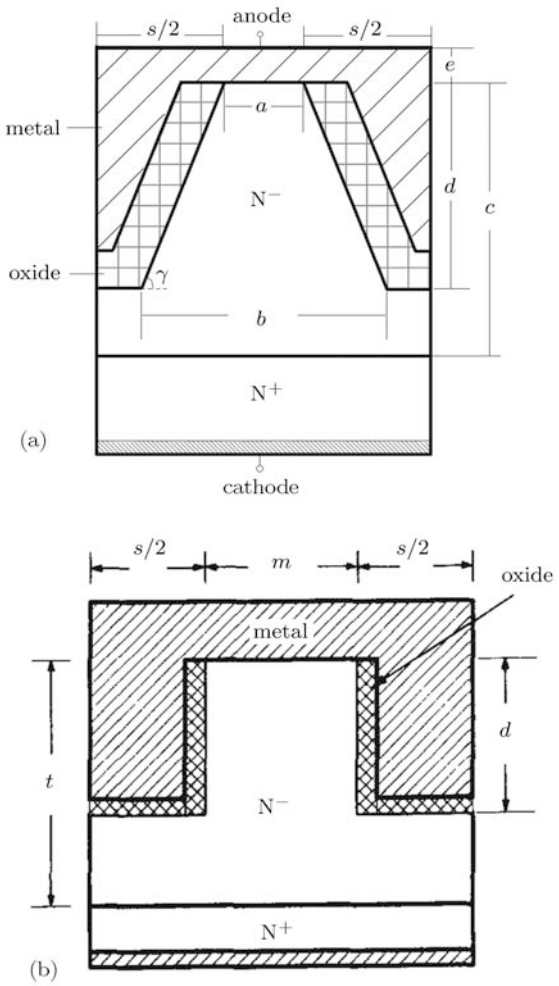


Fig. 1. (a) Cross section of a TM-TMBS cell, and (b) cross section of a TMBS cell.[9]

It has been discussed by Mehrotra *et al.* that in order to achieve a higher breakdown voltage while the reasonable forward voltage drop and the current carrying capability are maintained, the values of m, s, t, d, $t_{\rm ox}$, etc.[9] are chosen to be optimized. Similarly, in this work, the optimized structure of the TM-TMBS we found has the following parameters: $a = 0.8$ μm, $b = 3.16$ μm, $c = 8$ μm, $d = 5.9$ μm, $s = 4$ μm, $\tan\gamma = 5$ ($\gamma = 78.7°$), $t_{\rm ox} = 0.9$ μm, epi-layer doping $N = 1 \times 10^{16}$ cm^{-3}, and the Schottky barrier height (SBH) $\Phi_{\rm b0} = 0.782$ eV, which is equal to the SBH extracted from the measured I–V characteristics of a commercial planar SBD. The optimal TMBS structure, which is regarded as a comparative structure that has parameters as $m = 2$ μm, $s = 3$ μm and others are the same as those given above. In addition, a planar SBD structure, which is identical to the actual commercial one mentioned above, is also regarded as another comparative structure.

3. Results and discussion

3.1. Optimized TM-TMBS

In order to verify the expected reduction in field magnitude at the corner, a two-dimensional (2D) simulator APSYS[22] was used to analyse the structures.

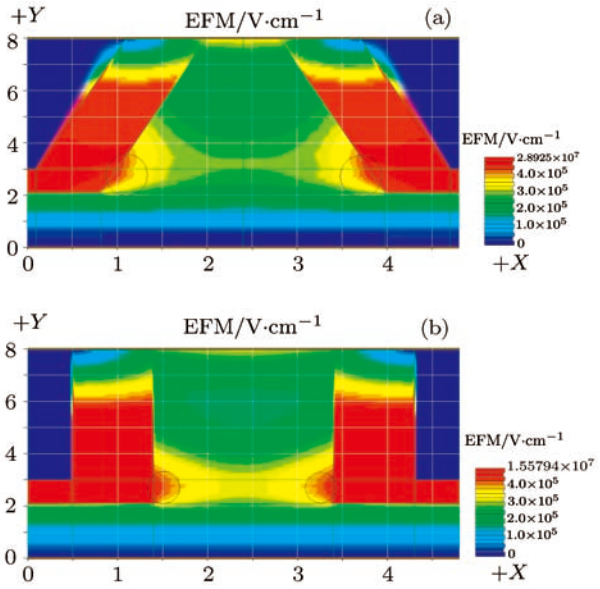


Fig. 2. 2D field distribution contours of (a) optimized TM-TMBS and (b) optimized TMBS at 170 V reverse bias. The electric field magnitude is abbreviated as EFM (in units V·cm^{-1}).

Figure 2 shows the 2D field distribution contours of (a) an optimized TM-TMBS and (b) an optimized TMBS under 170-V reverse bias, which is close but not high enough to cause breakdown. The field crowding at the corners of the MOS structure should be noticed. The maximum value of the field magnitude in N$^-$ Si, which is marked with a circle, is of the order of 4×10^5 V/cm. It is clear that a high field leads to impact ionization and thus avalanche breakdown. As shown in Eq. (1), the critical breakdown field magnitude for a one-sided step junction that has a doping concentration of 1×10^{16} cm^{-3} should be around 4×10^5 V/cm.[2] Therefore it can be inferred that this

area will be the main region where great impact ionization and then breakdown takes place when a higher reverse bias is applied,

$$E_{\rm m} = \frac{4 \times 10^5}{1 - (1/3)\lg(N/10^{16}\ {\rm cm}^{-3})}\ {\rm V/cm}. \quad (1)$$

Figure 3 demonstrates the field magnitude along both (a) the horizontal and (b) the bevel edges of the epi layer and along (c) the mesa central line, as shown in the insets. In Fig. 3, the devices are each under a 170-V reverse bias. One can see from Fig. 3 that the sharp field peak at the corner of the TMBS mesa region is eliminated in the TM-TMBS. Being contrary to the sharp needlepoint causing point discharge, the obtuse angle of metal prevents, or at least weakens, the so-called "field-crowding" effect there. It can be understood that the area under bevel edges burdens a higher voltage drop and reduces the field magnitude at the corner. For an extreme instance, if the tilt angle γ is 0°, then it will have no field crowding at the corner and the TM-TMBS is converted into a planar SBD, but it also gets no benefit from space charge coupling as the TMBS does. This phenomenon makes the TM-TMBS look like an eclectic mix of TMBS and planar SBD. This mix not only reduces the field magnitude at the contact surface, as the TMBS does, but also eliminates the field peak near the trench corner, which the TMBS has. Therefore, the TM-TMBS attains better reverse I–V characteristics, as shown below.

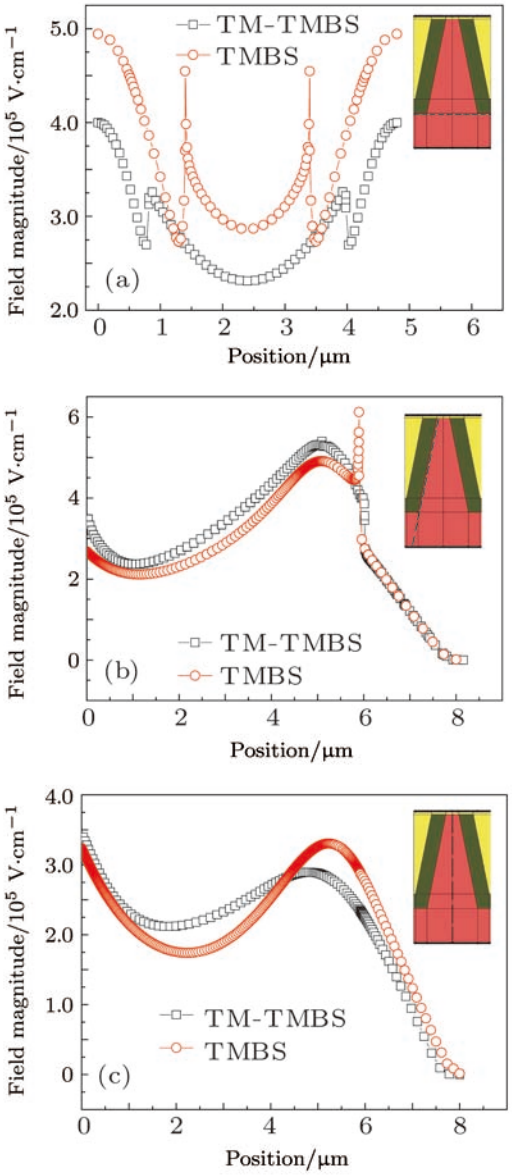


Fig. 3. Field distributions along (a) the horizontal edge (from left to right), (b) the bevel (vertical for the case of TMBS) edge of the N^- epi layer (from top to bottom), and (c) the mesa central line (from top to bottom) at 170-V reverse bias.

Figure 4 demonstrates the reverse I–V characteristics of the TM-TMBS, TMBS, and planar SBD. The current is divided by the area occupied on the wafer rather than the actual conducting area. One can see from Fig. 4 that the breakdown voltage of the TM-TMBS is 186 V, 6.3% higher than that of the TMBS while the leakage current is 4.3×10^{-6} A·cm^{-2} (e.g. at 140-V bias), around 26% smaller. These can be understood due to the reduction in field magnitude at the trench corner and a more "uniform" field distribution in the N^- depletion region.

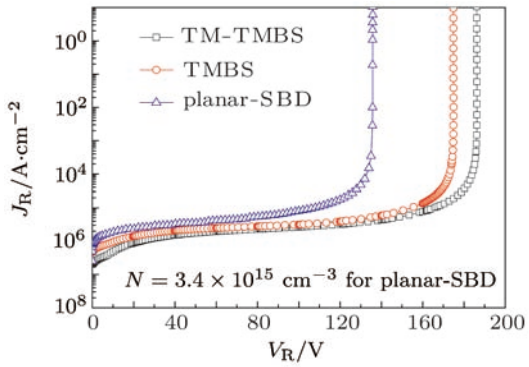


Fig. 4. Reverse I–V characteristics of TM-TMBS, TMBS, and planar SBD.

Figures 5(a) and 5(b) demonstrate the overview and detailed view of the forward I–V characteristics of the TM-TMBS, TMBS, and planar SBD. The current is divided by the area occupied on the wafer rather than the actual conducting area. One can see from Fig. 5(b) that the TM-TMBS has a 0.05-V larger forward voltage drop at 180 A/cm^2 than TMBS. This is an acceptable degradation compared with the improvement in reverse characteristics. In addition, the smaller slope also indicates a larger resistance. These

can be understood due to the reduction in conducting area compared with the TMBS structure.

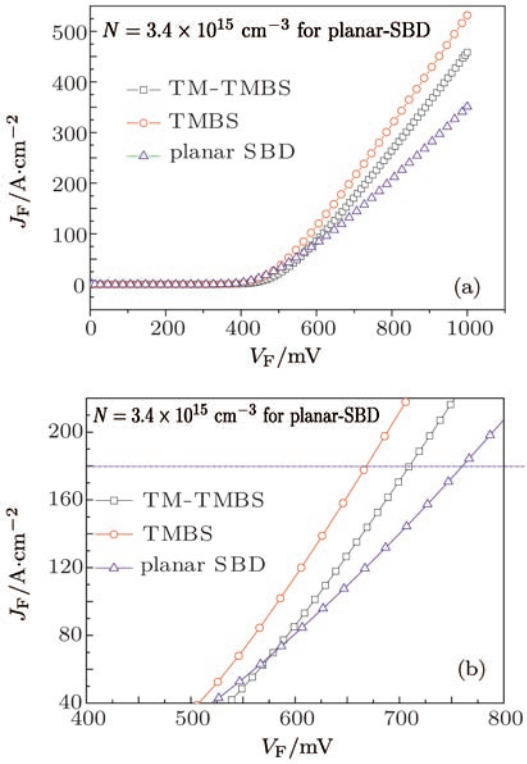


Fig. 5. (a) Overview and (b) detailed view of forward I–V characteristics of TM-TMBS, TMBS, and planar SBD.

3.2. Parametric variation

In order to verify if this TM-TMBS structure is the optimum one, some parameters, including mesa top width a, tilt angle γ, oxide thickness t_{ox}, and trench depth d, are varied and studied one by one while keeping the others constant. The relationship between breakdown voltage and these parameters is revealed below.

Figure 6 demonstrates the relationship between breakdown voltage and mesa top width a. It can be seen from Fig. 6 that there is an optimal value $a = 0.8$ μm.

Figure 7 shows the 2D field distribution contour of the TM-TMBS with $a = 2$ μm, at 140-V reverse bias. Figure 8 shows the field distribution magnitudes along the mesa central line, from top to bottom, at 160-V reverse bias for $a = 0.2$ μm and $a = 0.8$ μm, and 140 V for $a = 2$ μm. It is easy to understand that with a larger a, the mesa region is harder to pinch off, so the TM-TMBS behaves more like a planar SBD, which has a triangular shape field distribution along the mesa central line. Actually, combining Fig. 7 and Fig. 8, one can notice that for $a = 2$ μm, the field peak is located at the top semiconductor-metal contact of the mesa central line, rather than at the corner, resembling the case of the planar SBD. As figure 6 shows, the breakdown voltage for $a = 2$ μm is 148 V, 38 V smaller than that for $a = 0.8$ μm.

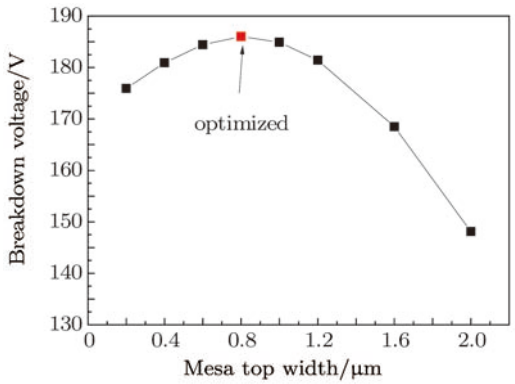


Fig. 6. Breakdown voltage as a function of mesa top width a.

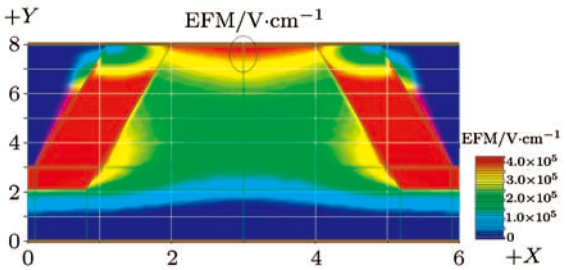


Fig. 7. The 2D field distribution contour of the TM-TMBS with $a = 2$ μm, at 140-V reverse bias.

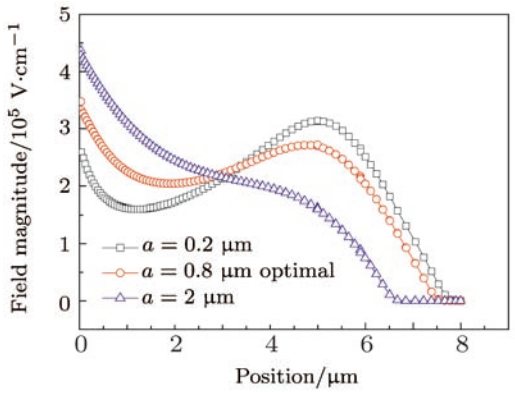


Fig. 8. Field distributions along the mesa central line, from top to bottom, at 160-V reverse bias for $a = 0.2$ μm and $a = 0.8$ μm, and 140 V for $a = 2$ μm.

In contrast, if a is smaller than an optimal value, the trapezoid mesa region becomes fully pinched off at a relatively smaller bias. Figure 9 shows the 2D field distribution contour of the TM-TMBS, with $a = 0.2$ μm, at 160-V reverse bias. Figure 10 shows the field distributions along the bevel edge, from top to bottom, at 160-V reverse bias for $a = 0.2$ μm and $a = 0.8$ μm, 140 V for $a = 2$ μm. After the mesa

region is prematurely pinched off, the additional biased voltage is burdened mainly by the circle-marked region in Fig. 9, forming a higher electric field peak there, as figures 9 and 10 demonstrate. It may be called "over pinched-off". It can be seen in Fig. 10 that the field peak value for $a = 0.2$ μm is about 2% larger than that for $a = 0.8$ μm, and consequently the breakdown voltage for $a = 0.2$ μm (176 V) is about 5% smaller than that for $a = 0.8$ μm (186 V).

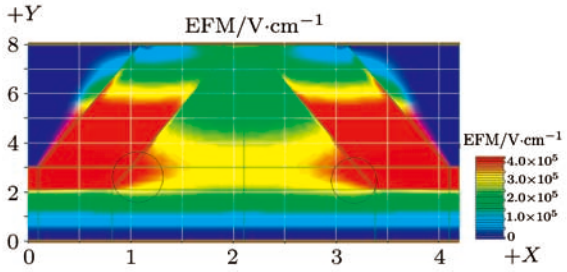


Fig. 9. The 2D field distribution contour of the TM-TMBS with $a = 0.2$ μm, at 160-V reverse bias.

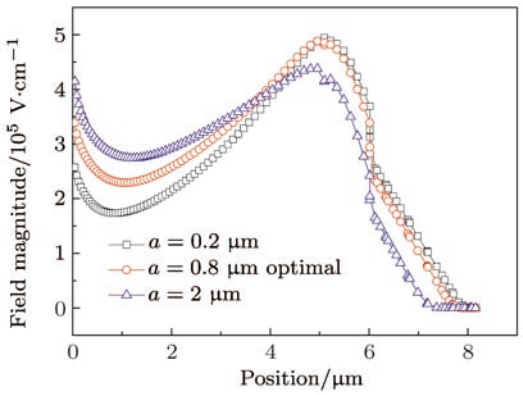


Fig. 10. Field distributions along the bevel edge, from top to bottom, at 160-V reverse bias for $a = 0.2$ μm and $a = 0.8$ μm, 140 V for $a = 2$ μm.

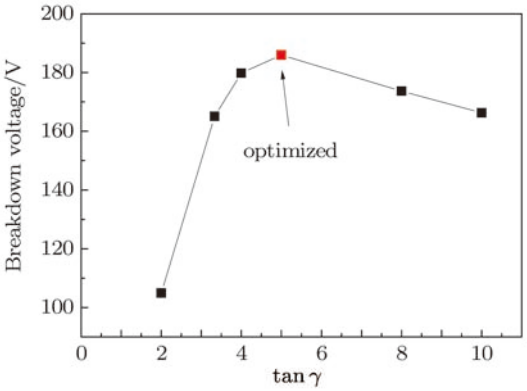


Fig. 11. Breakdown voltage as a function of tangent tilt angle tan γ.

Figure 11 demonstrates the relationship between breakdown voltage and tangent tilt angle γ. It can be seen that there is an optimal value tan $\gamma = 5$ (corresponding to $\gamma = 78.7°$).

Given a large tan γ, say, 10 (corresponding to $\gamma = 84.3°$), the device behaves more like a regular TMBS (corresponding to $\gamma = 90°$), which has a sharp field peak near the corner, thus obtaining a smaller breakdown voltage as already discussed in Subsection 3.1.

In contrast, given a small tan γ, the mesa bottom is too wide to be pinched off, thus obtaining a field distribution more like a planar SBD. Figure 12 shows the 2D field distribution contour of TM-TMBS with tan $\gamma = 2$ (corresponding to $\gamma = 63.4°$), at 80-V reverse bias. Figure 13 shows the field distribution along the mesa center line, from top to bottom, at 80-V reverse bias. As can be seen from Fig. 12, the mesa bottom width b is about 6.7 μm, which is much wider than the optimal value 3.16 μm, due to the difference in γ. Given such a large b, the mesa bottom is not completely depleted and pinched off under 80-V reverse bias. Therefore, the field distribution along the mesa central line is still a triangular shape that resembles that of a planar SBD, as shown in Fig. 13. Consequently, the breakdown voltage is only 105 V for tan $\gamma = 2$, 81 V less than that of the optimal structure.

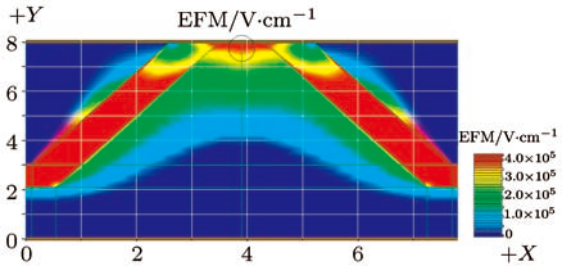


Fig. 12. The 2D field distribution contour of the TM-TMBS with tan $\gamma = 2$, at 80-V reverse bias.

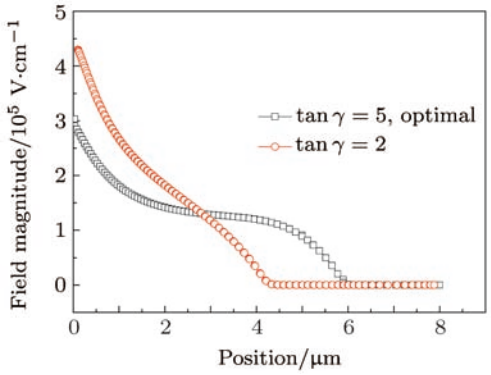


Fig. 13. Field distributions along the mesa central line, from top to bottom, at 80-V reverse bias.

Figure 14 demonstrates the relationship between breakdown voltage and oxide thickness t_{ox}. It can be

seen that there is an optimal value $t_{ox} = 0.9$ μm.

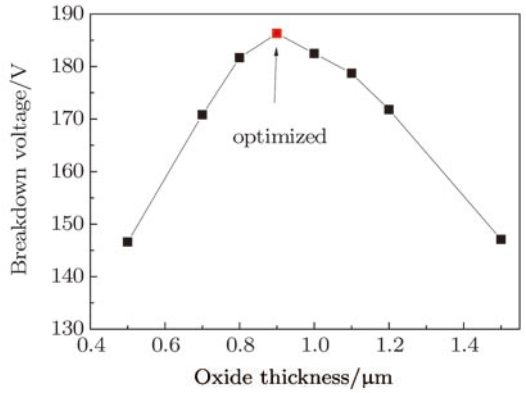


Fig. 14. Breakdown voltage as a function of oxide thickness t_{ox}.

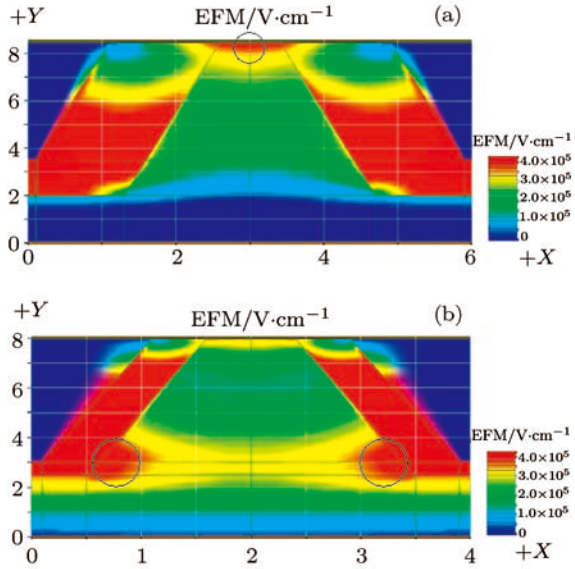


Fig. 15. The 2D field distribution contours of the TM-TMBS with (a) $t_{ox} = 1.5$ μm, and (b) $t_{ox} = 0.5$ μm, at 140-V reverse bias.

Because t_{ox} determines the capacitance and thus the capability of pinching off the mesa region, it is reasonable to expect large t_{ox} to lead to a weak pinch-off effect while small t_{ox} lead to premature pinching off or "over pinching off", which is similar to the case where the device has a small a, as discussed above. Figure 15 shows the 2D field distribution contours of the TM-TMBS with (a) $t_{ox} = 1.5$ μm, (b) $t_{ox} = 0.5$ μm, at 140-V reverse bias. Figure 16 shows the field distribution along (a) the mesa central line and (b) the bevel edge, from top to bottom, at 140-V reverse bias. The field distribution comparison is also similar to the discussion of mesa width a. Actually, with a pretty large $t_{ox} = 1.5$ μm, due to the small oxide capacitance and thus poor ability to deplete and pinch off the mesa region, the TM-TMBS has a field peak at the top Schottky contact and a triangular shape field distribution like a planar SBD, as shown in Figs. 15(a) and 16(a). In contrast, with a small $t_{ox} = 0.5$ μm, due to a much stronger "over pinched-off" effect, the TM-TMBS has an unusual high field peak at the trench corner, as shown in Figs. 15(b) and 16(b). The breakdown voltage is less than 150 V for both $t_{ox} = 1.5$ μm and $t_{ox} = 0.5$ μm.

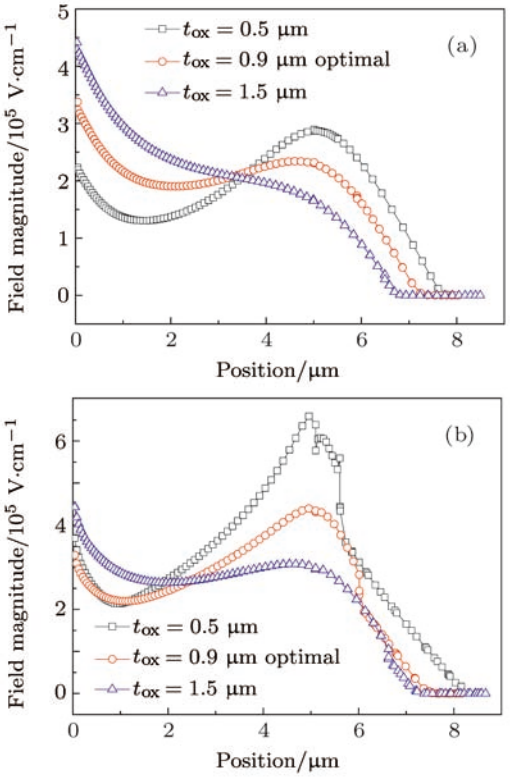


Fig. 16. Field distribution along (a) the mesa central line and (b) the bevel edge, from top to bottom, at 140-V reverse bias.

From the above discussion about a, γ, and t_{ox}, one can conclude two rules in common. One is that the mesa region should be designed to be pinched off under a reasonable bias, so that the field distribution can be modulated to be different from a triangular one of planar SBD. In particular, the field magnitude at the contact surface will be greatly reduced. The other is that the mesa region should be designed so that it can avoid being over pinched off under a relatively small bias. Therefore the field magnitude at the bottom corner of the mesa region will not be too large.

The case of trench depth d is a little different from the cases of the above three parameters.

Figure 17 demonstrates the relationship between breakdown voltage and trench depth d. Figure 18

shows the forward I–V characteristics of the TM-TMBS with different trench depths and a planar SBD. Figure 19 shows the 2D field distribution contour of the TM-TMBS with $d = 1.9$ μm, at 60-V reverse bias. Figure 20 exhibits the field distribution along the mesa central line, from top to bottom, at 60-V reverse bias. It can be seen in Fig. 17 that with an "optimal" $d = 5.9$ μm, the device does not obtain the highest breakdown voltage. The reason for choosing this value to be optimal is that a larger d leads to larger series resistance, which negatively influences the forward performance of the device, while smaller d leads to a smaller mesa area being pinched off, obtaining a smaller breakdown voltage. For the former case, one can see that with $d = 10.9$ μm, the breakdown voltage reaches 228 V due to the additional depth, which burdens a higher voltage drop, but as shown in Fig. 18, the device performance is even worse than that of a conventional planar SBD under forward bias, hence making it unacceptable. For the latter one, as shown in

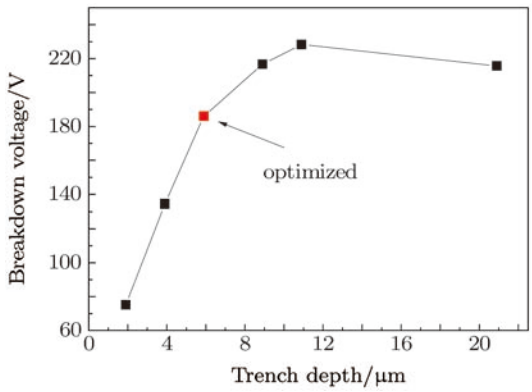


Fig. 17. Breakdown voltage as a function of trench depth d.

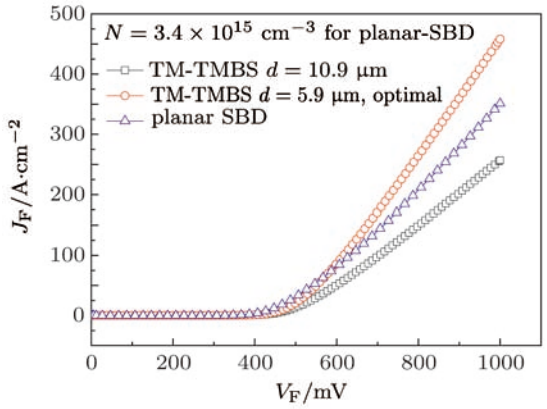


Fig. 18. Forward I–V characteristics of the TM-TMBS with different trench depths and a planar SBD.

Figs. 19 and 20, one can see that with a pretty small $d = 1.9$ μm, the mesa region area that is fully depleted is relatively small. This area affects the field distribution so little that the TM-TMBS still has a triangular sfield distribution like a planar SBD. Consequently, the breakdown voltage is only 75 V.

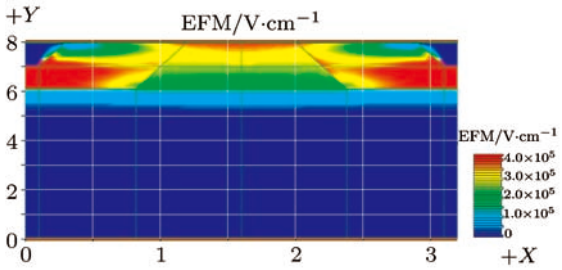


Fig. 19. The 2D field distribution contour of the TM-TMBS with $d = 1.9$ μm, at 60-V reverse bias.

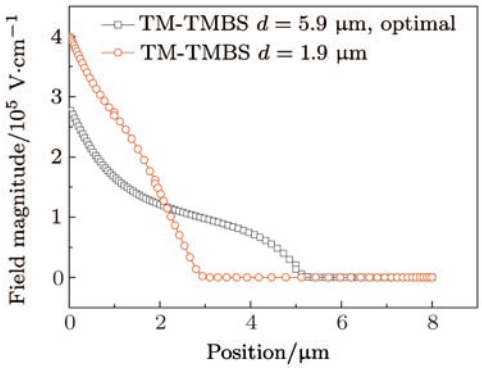


Fig. 20. Field distributions along the mesa central line, from top to bottom, at 60-V reverse bias.

It is worth mentioning that although only theoretical simulation is carried out in this work, it is feasible to fabricate a TM-TMBS. The key process for such a device is to etch an angled trench in a Si substrate. According to the results reported by Carlile *et al.*,[23] a trench sidewall with an angle tilting from 32° to 7° can be obtained by varying the substrate temperature from 40 °C to 190 °C in a reactive ion etching process. In other words, a tilt angle γ, defined in our work, ranging from 58° to 83°, can be achieved with a proper etch process. And one may notice that the optimal γ, 78.7° that we suggested, is located within the range.

4. Conclusion

In this paper, an improved structure of a rectifier TM-TMBS is proposed. The key feature of the TM-TMBS is the trapezoid mesa region, which leads to tilted MOS sidewalls compared with the rectangular mesa region of the TMBS. By restraining the

field magnitude peak near the trench corner, the TM-TMBS achieves better reverse I–V characteristics, including a breakdown voltage of 186 V, which is 6.3% higher and a leakage current 4.3×10^{-6} A/cm^2, which is 26% lower than that of a regular TMBS, though it demonstrates slightly weaker forward performance.

Different parameters of the TM-TMBS, including mesa top width a, tilt angle γ, oxide thickness $t_{\rm ox}$, and trench depth d, are varied and simulated while keeping the others constant. The results show that there are optimal values as $a = 0.8$ μm, $\tan\gamma = 5$, $t_{\rm ox} = 0.9$ μm, and $d = 5.9$ μm. Furthermore, the relationship between breakdown voltage and these parameters is revealed and explained. Design rules are given according to the relationship.

Acknowledgement

The authors would like to thank Dr. Simon Li of Crosslight Software Inc. for his helpful discussion.

References

[1] Baliga B J 1995 *Power Semiconductor Devices* (Pacific Grove: PWS)

[2] Sze S M and Ng K K 2007 *Physics of Semiconductor Devices* 3rd edn. (Hoboken: Wiley-Interscience)

[3] Baliga B J 1984 *IEEE Electron Device Lett.* **5** 194

[4] Baliga B J 1985 *Solid-State Electronics* **28** 1089

[5] Song Q W, Zhang Y M, Zhang Y M, Zhang Q and Lü H L 2010 *Chin. Phys.* B **19** 087202

[6] Nan Y G, Pu H B, Cao L and Ren J 2010 *Chin. Phys.* B **19** 107304

[7] Baliga B J 1987 *IEEE Electron Device Lett.* **8** 407

[8] Song Q W, Zhang Y M, Zhang Y M, Zhang Q, Guo H, Li Z Y and Wang Z X 2010 *Chin. Phys.* B **19** 047201

[9] Mehrotra M and Baliga B J 1995 *Solid-State Electronics* **38** 801

[10] Sakai T, Matsumoto S and Yachi T 1998 *ISPSD'98: Proceedings of the 10th International Symposium on Power Semiconductor Devices & ICs* June 3–6, 1998, Kyoto, Japan p. 293

[11] Mahalingam S and Baliga B J 1999 *Solid-State Electronics* **43** 1

[12] Khemka V, Ananthan V and Chow T P 2000 *IEEE Electron Device Lett.* **21** 286

[13] Shimizu T, Kunori S, Kitada M and Sugai A 2001 *ISPSD'01: Proceedings of the 13rd International Symposium on Power Semiconductor Devices & ICs* June 4–7, 2001 Osaka, Japan p. 243

[14] Moon J W, Choi Y I and Chung S K 2002 *Proceedings of 23rd International Conference on Microelectronics* May 12–15, 2002 Nis, Yugoslavia p. 189

[15] Juang M H, Yu J, Hwang C C, Shye D C and Wang J L 2010 *Microelectronics Reliability* **51** 365

[16] Juang M H, Yu J and Jang S L 2010 *Current Appl. Phys.* **11** 698

[17] Schoen K J, Henning J P, Woodall J M, Cooper J A and Melloch M R 1998 *IEEE Electron Device Lett.* **19** 97

[18] Roccaforte F, La Via F, Di Franco S and Raineri V 2002 *Appl. Phys. Lett.* **81** 1125

[19] Roccaforte F, La Via F, La Magna A, Di Franco S and Raineri V 2003 *IEEE Transactions on Electron Devices* **50** 1741

[20] Li W Y, Ru G P, Jiang Y L and Ruan G 2010 *ICSICT'10: Proceedings of the 10th International Conference on Solid-State and Integrated Circuit Technology* November 1–4, p. 1789

[21] Thapar N and Baliga B J 1997 *Solid-State Electronics* **41** 1929

[22] *Crosslight Device Simulation Software—General Manual* 2010.07 Crosslight Software Inc. Burnaby

[23] Carlile R N, Liang V C, Palusinski O A and Smadi M M 1988 *J. Electrochem. Soc.* **135** 2058